Proceedings of the
Annual Stability Conference
Structural Stability Research Council
Orlando, Florida, April 12-15, 2016

Axial stability of columns composed of combined sigma CFS

M El. Aghoury[1], M.T. Hanna[2], E.A.Amoush[3]

Abstract

Recently, using of cold formed steel sections in constructions have shown rapid growth due to their lightness, high strength and stiffness, fast and easy erection. Generally, Cold-formed steel sections are shaped to suit the particular application. Lipped channel sections are the most used sections, however, sigma sections need more effort in fabrication but they have high strength-weight ratios compared with the lipped channel sections. This study presents series of compression tests on columns that are composed of combined back to back sigma CFS. Eight specimens varied in their plate element width-thickness ratios, and covered different member slenderness ratios were tested. columns were assembled by means of bolts. Measurements of residual stresses and geometrical imperfections were carried out. Moreover, the specimens were simulated by a finite element model using shell element that accounts for both geometric and material non-linearties. The measured geometric imperfections and residual stresses were included in the numerical model. The elastic critical buckling shape that obtained by the eigen value analysis was scaled to the desired geometric imperfection values, then this imperfect shape is used as starting point of the nonlinear analysis. Finally, the test results have been compared with those of non-linear finite element model, and also with the predicted ultimate strengths determined by the American AISI, and DSM specifications. Results reflect that there is good agreement between the experimental and the FEM results. Moreover, the AISI and DSM can reasonably predicate the ultimate loads of such sections.

1. Introduction

Due to the high strength weight ratios, simple, and fast erection procedures of steel cold formed sections, their applications as structural members have been extended. They are used not only as stud members in load bearing wall panels but can also employed as column or beams in moderate span frames. However, in frames it might be required to combine the section together either back to back "I" or toe to toe "box" section. The axial compression capacity of combined members is more than twice that of the individual members. Design codes have some provisions for the spacing between fasteners, and the modified slenderness ratios to account for the effect of

[1]Professor, Faculty of Engineering, Ain Shams University, Egypt, aghoury_tc@yahoo.com
[2]Professor, Housing and Building National Research Center, Egypt, m_tawfick2003@yahoo.com
[3]Assistant Professor, Higher Technological Institute, essamamoush2008@yahoo.com

shear deformation on the overall flexural buckling of such members. However, buckling of cold formed sections involves different complicated modes like local, and distortional buckling. Therefore, this research aims to study structural behavior of columns composed of two sigma CFS connected back to back by bolts. The study includes the effect of cross section geometric proportions, overall slenderness ratios, and the spacing between fasteners on the axial capacity of combined columns. In these columns the different modes of failure are: (1) sectional buckling (either local or distortional), (2) interactive sectional – overall buckling, (3) overall buckling. The maximum carrying capacity of the members is reached when one of the previous modes of failure happened. Experimental and theoretical investigations have been performed. Finally, comparison of experimental results with those of finite element and standard codes were carried out.

Several researches have been done in this field. Thomas H. K. Kang et al., (2013) investigated the different buckling modes of built up cold-formed steel columns. They tested 42 columns and determined the effects of the geometrical properties such as thickness and width of the members on their axial strength. David C. Fratamic et al., (2015) employed a small two-dimensional beam finite element model in static and eigen-buckling analysis to explore the behavior of cold-formed steel built-up sections in global flexural buckling. The model includes two-dimensional beam finite element model connected by a special fastener element. H.H. Lau and T.C.H. Ting (2009) investigated the compressive capacity of pin-ended cold-formed steel built-up I sections using the finite element method (FEM). They used two identical channels sections oriented back to back forming an I-shaped cross section and connected to each other at certain spacing along their length. Their results showed that the effective width method and direct strength method were generally conservative for cold-formed steel built-up I sections. Fadhluhartini Muftah et al., (2014) found that, the bolt arrangement was important in making sure the combine CFS columns can achieve the full sectional strength. They suggested that the position of the screw near to the end help the column to act as a full section without premature failure at the end bearing. Eventually, they recommended that, the used of bolt near the end at end distance about 20 mm are very effective to avoid end bearing failure. Mohamed El Aghoury et al., (2014) found that the ultimate strength of axially loaded single sigma CFS decreases by increasing the overall imperfection. In-addition the residual stresses reduce the ultimate strength of the columns by about 4.0%, and the predicted design loads by AISI-2007, and DSM are conservative. D.J Klingshirn, et al. (2010), tested fifty-eight sigma shaped Specimens under axial compressive load at various lengths to study global, distortional, and local buckling failure modes. Also, they compare their results with the AISI-2007 design methods, Effective Width Method (EWM) and Direct Strength Method (DSM). Andrzej Garstecki et al. (2002) studied the distribution and intensity of the initial imperfections to be used in the generation of FEM of imperfect steel structures as a starting point for nonlinear analysis accounting for initial imperfections. Also, they compared the imperfections with the linear buckling modes, and limit values of imperfections were evaluated using the statistical analysis based on Gauss distribution. M. El Aghoury, et al., (2010) measured the geometrical as well as the residual stresses in battened columns composed of four equal cold formed angles, and they found that the angle local geometric imperfections range from b/50 to b/20, where b is the flat width of the angle leg, while the column overall geometric imperfections ranged from L/1600 to L/284. In addition, the maximum compressive membrane strain is at the corner of the section and can be as high as 850 μs and the maximum tensile membrane strains were about 400 μs.

2. Experimental Work

2.1Section Size

The tested columns are composed of two sigma CFS. The sections are assembled back to back by bolts at the mid height of the column. Each sigma section has 160mm overall web depth, H. The middle part, H3, of the web is kept constant equal to 40mm, while the remaining parts, H1&H2, are changed to achieve two ratios of the inward recess of the middle part of the web, a, to the flange width, B, a/B = 0.25 & 0.75. Two flange widths, B, are selected which are equal to 40mm and 50mm, and the lip depth is equal to 13.3mm. This means that the lip depth to flange width ratios, D/B, are equal to 0.33, 0.267. The section thickness is set equal to 1 mm. Dimensions of the tested specimens are listed in Table (1).

Table 1: Test specimen dimensions

Specimen	Section Dimensions (mm)							L (mm)
	H	H1	H2	H3	B	D	a	
S40-25-50	160	50	10	40	40	13.3	10	895
S40-25-100	160	50	10	40	40	13.3	10	1788
S40-75-50	160	30	30	40	40	13.3	30	1125
S40-75-50	160	30	30	40	40	13.3	30	2250
S50-25-50	160	47.5	12.5	40	50	13.3	12.5	1140
S50-25-100	160	47.5	12.5	40	50	13.3	12.5	2282
S50-75-50	160	30	30	40	50	13.3	30	1142
S50-75-100	160	30	30	40	50	13.3	30	2500

Note, L is the height of the specimens

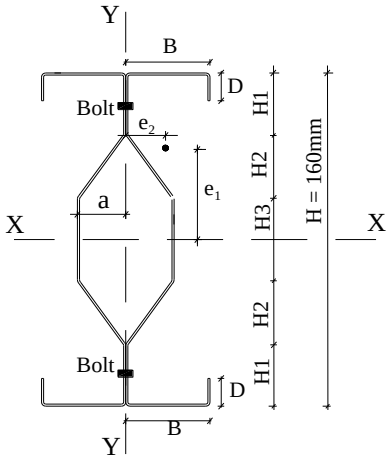

Fig.1: Cross Section Dimensions

2.2 Test Setup and Results

The specimens were aligned vertically in the test frame as shown in Fig. 2. The loads were applied at the upper end by a 250 KN jack, while the lower end resists the developed reactions. To ensure equal stresses distribution across the section, two 20 mm thick plates were connected at the ends of each specimen by bolts. In addition, the ends of each specimen were milled flat to ensure full contact between specimens and end bearing plates. The loads were applied to the specimens through hinges placed in a groove made in the thick end plates. These end conditions allow rotation about strong and weak axis, while it prevents any horizontal displacement of the specimen. Moreover, the presence of head plates prevents the warping deformations of the specimens end sections. Bolts used in assembling the specimens and connecting them to the end plates were M6 H.S.B of Grade 8.8. Although theodolite was used to measure the verticality of the specimen in the test frame, there were some eccentricities at the ends of all specimens. Detailed measurements of eccentricities at specimen ends (e_1 & e_2) were recorded in the laboratory and listed in Table 3.

Specimen

LVDT at the mid height section

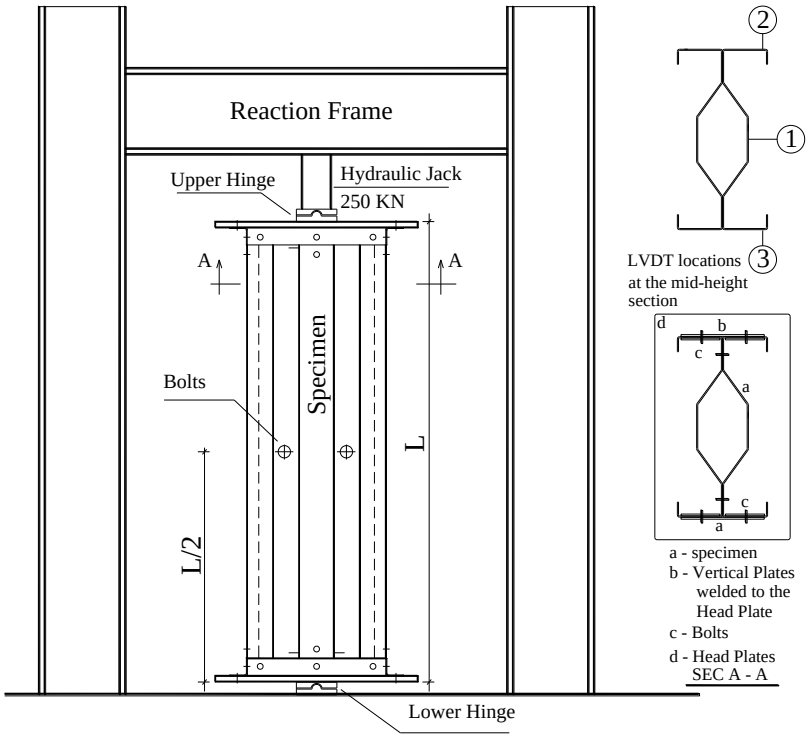

Schematic diagram for the test setup

Figure 2 Test setup

The load axial shortening and lateral displacement were recorded by using the Tokyo-Sokki S-2420 data acquisition system. Three (LVDT) transducers were placed at the specimen mid height to measure the horizontal displacements of the web mid points and the flange-lip juncture points. In addition, one (LVDT), was attached vertically to measure the axial shortening. At the beginning of the test, 1/10 of the estimated ultimate loads was applied as initial load. This load was kept constant for about 10 seconds to achieve full contact between the load jack and the specimen end bearing plate. Tensile coupons were prepared and tested according to the ASTM-A370, results revel that the steel is mild steel with yield stresses and Young's modulus equal to 240MPa, and 200000 MPa; respectively.

In this work, the geometric imperfections were measured for 16 specimens using a dial gauge with an accuracy of 0.01 mm. Local imperfections, δ_L, demonstrate the out of flatness in the plate elements forming the section, and it is calculated by subtracting the readings taken at the middle points from the average of the readings at the two end points of each plate elements. However, distortional imperfections, δ_d, reflect the translation of one plate end with respect to the other end. Further, shifting of the imperfect section centroid from the original member axis represents the overall imperfection values, Δ. It is found that, the average local imperfections, δ_L, is 0.38t, while the average distortional imperfections, δ_d, is 0.28t. In addition, the average overall geometric imperfections, Δ, is L/1000. Further, details of residual stresses measurements are illustrated in Mohamed El Aghoury, et.,al. (2014). The measured patterns are characterized by tensile strains concentrated at the corners and compressive strains spread on the middle zone of each flat part of the section, see Fig. 3.

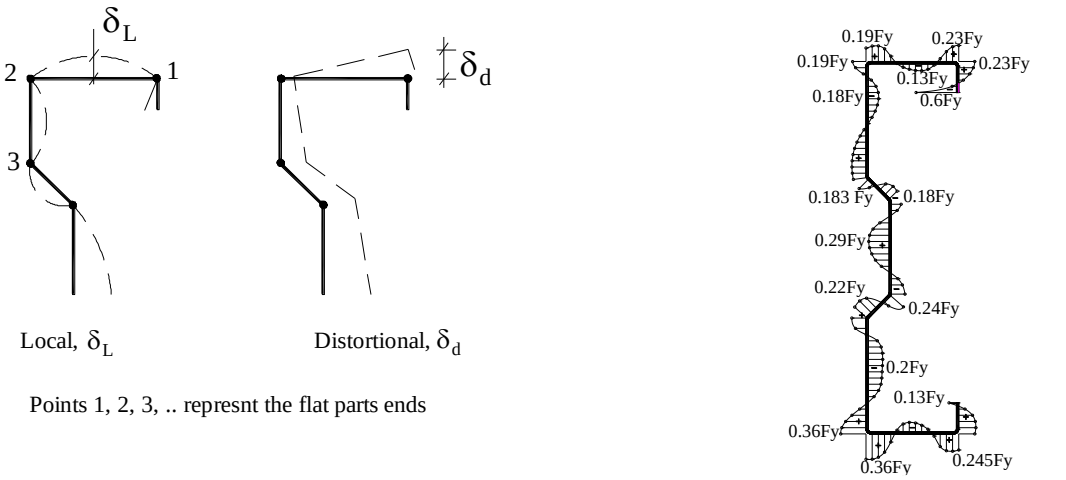

a) Local and Distortional imperfections b) Residual stresses pattern

Figure 3 Initial imperfections pattern

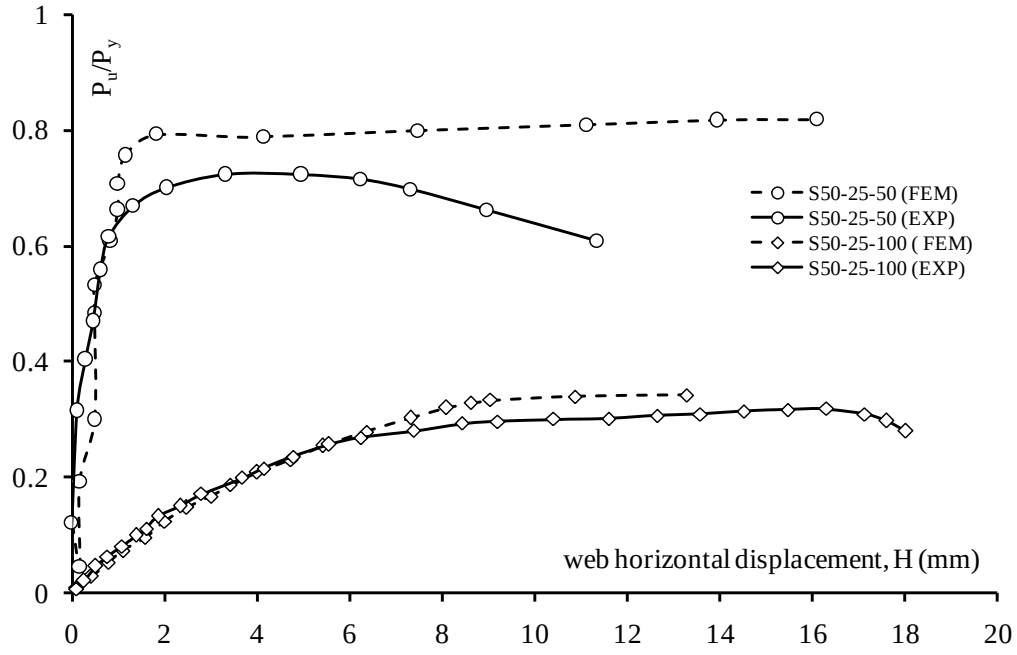

Figure 4 Load-horizontal displacements of specimens S50-25-50 & S50-25-100

The applied loads, P, are normalized with respect to the squash load, $P_y = A_f F_y$, and plotted versus the horizontal displacement, H, of the web mid point, and the axial shortening in Fig. 4 and Fig. 5; respectively. Note, A_f indicates the gross section area. At the early stage of loading, the columns response is almost linear tell distortional buckling waves are happened in the flanges, then the horizontal displacements are obviously increased, and the column stiffiness decreased continuously up to failure. The experimental ultimate loads of the tested specimens are listed in Table 3.

Generally, in cold formed sections there are three basic failure modes which are local buckling that involves rotation at internal folds, distortional buckling that involves both rotation and translation of internal fold lines, and overall buckling that involves "rigid-body" deformation of the cross-section without distortion. From this aspect, the deformed shapes observed can be regarded as distortional buckling for short columns. However, in long columns the mode of failure is overall bending in addition to distortional buckling in flanges. The distortional buckling half waves length measured are 500mm and 650mm for specimens S50-75-100 and S50-25-100; respectively. Further the middle section of short columns exhibit yielding in some parts. Figure 6 illustrate the failure modes of specimens S50-25-50 & S50-25-100.

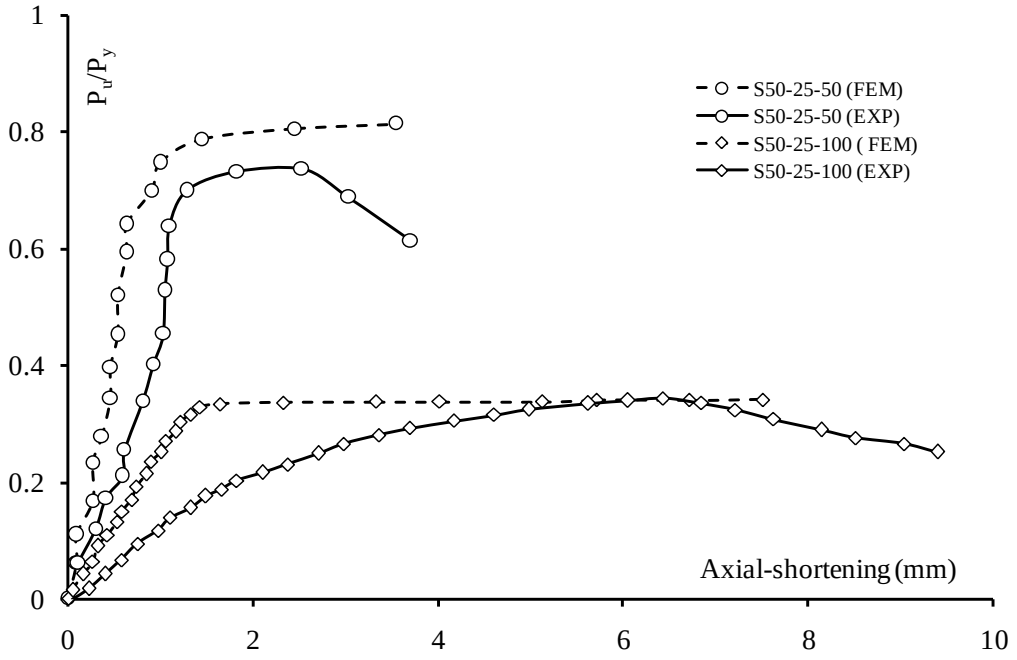

Figure 5 Load-axial shortening of specimens S50-25-50 & S50-25-100

Table 3: Test Results

Specimen	λ_c	a/B	D/B	e_1 (mm)	e_2 (mm)	Pu (KN)					
						Experimental		FEM			
						P_u	P_u/P_y	P_{u1}	P_{u1}/Py	P_{u2}	P_{u2}/Py
S40-25-50	0.68	0.25	0.33	12	25	68	0.52	73	0.56	118	0.91
S40-25-100	1.37	0.25	0.33	----	----	57	0.43	61.9	0.47	61.8	0.47
S40-75-50	0.88	0.75	0.33	----	----	102	0.74	115	0.83	115	0.84
S40-75-100	1.77	0.75	0.33	20	----	57	0.41	57	0.41	84	0.61
S50-25-50	0.7	0.25	0.26	----	----	102	0.72	112.6	0.8	112	0.8
S50-25-100	1.4	0.25	0.26	8	25	48	0.34	48	0.34	63.5	0.45
S50-75-50	0.7	0.75	0.26	18	----	93	0.63	93.5	0.63	126	0.86
S50-75-100	1.55	0.75	0.26	----	----	60	0.4	64.2	0.43	64.2	0.43

Note, P_{u1} : Ultimate loads considering eccentricities e1 & e2
P_{u2} : Ultimate loads neglecting eccentricities e1 & e2

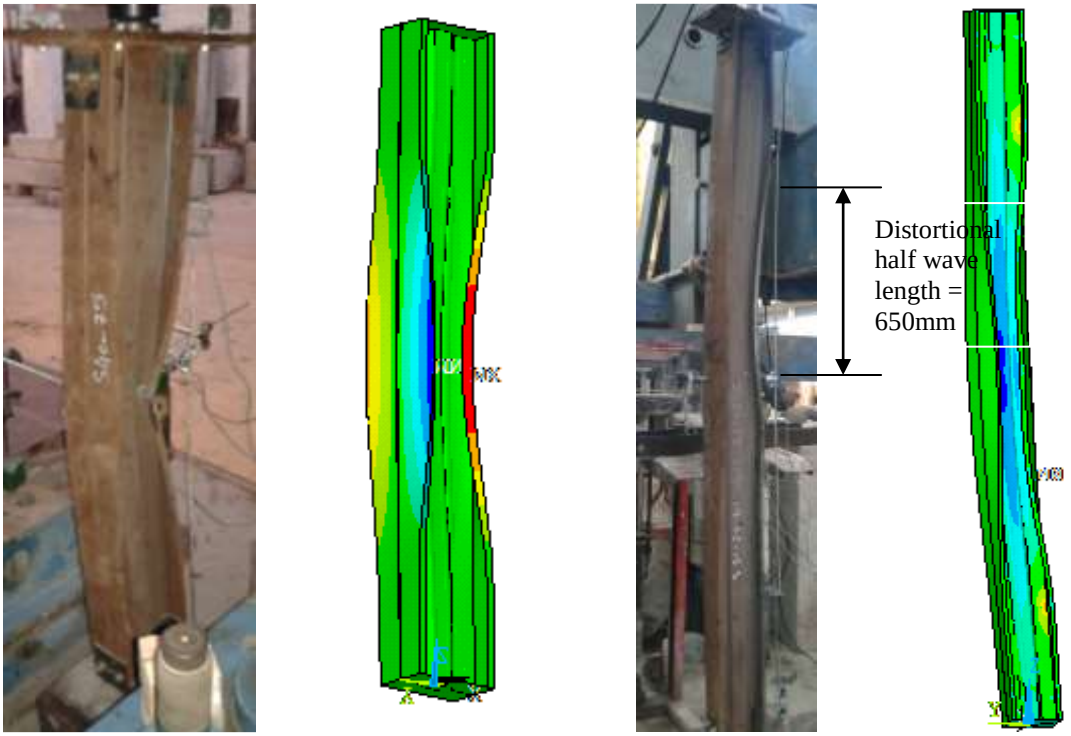

Figure 6 Failure modes of specimens S50-25-50 & S50-25-100

3. Numerical Simulation

The tested specimens were simulated by a three-dimensional (3D) finite element model. The modeling was conducted using the general purpose finite element software package ANSYS12.0.1. The non-linearity considered in the elasto-plastic finite element analysis was due to both geometrical and material non-linearities. The beams were modeled using 4-node shell element, SHELL181. This element has six degrees of freedom at each node, 3 translations and 3 rotations, to allow for the explicit simulation of the various buckling deformed shapes. Besides, SHELL181 is suitable for modeling thin to moderately-thick shell structures with both elastic and elasto-plastic material behaviors. To provide adequate accuracy, the element aspect ratio was kept nearly equal to one in the mesh. In addition, bolts that connect the webs are modeled using the contact element CONTA178. This element is capable of supporting compression in the contact normal direction and friction in the tangential direction.

ANSYS classical metal plasticity model was used to include the material non-linearity effects. This model implements the von-Mises yield surface to define isotropic yielding and associated plastic flow theory. A perfect plasticity model based on a simplified bilinear stress-strain curve without strain hardening was assumed. The elastic modulus of elasticity and yield stress of the steel material were considered as 210000 MPa and 240 MPa; respectively. The shear modulus was equal to 81000 MPa. Figure 7 shows the finite element model, loads, and boundary conditions.

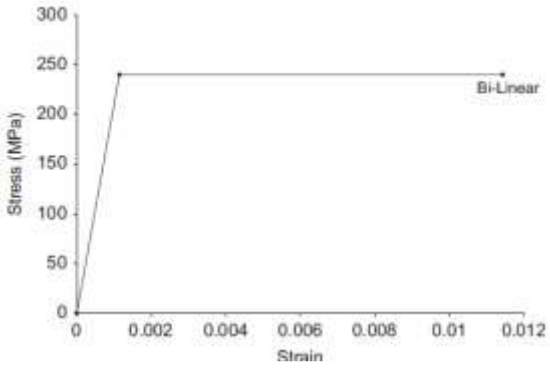

a) Idealized stress-strain curve

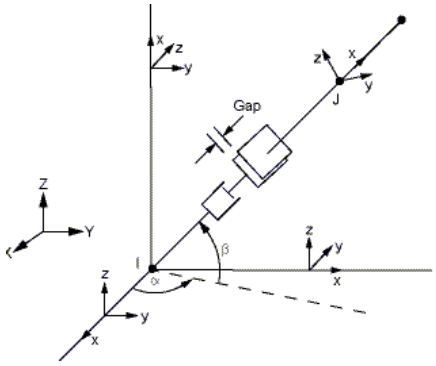

c) CONTA 178 element used to represent the fastener

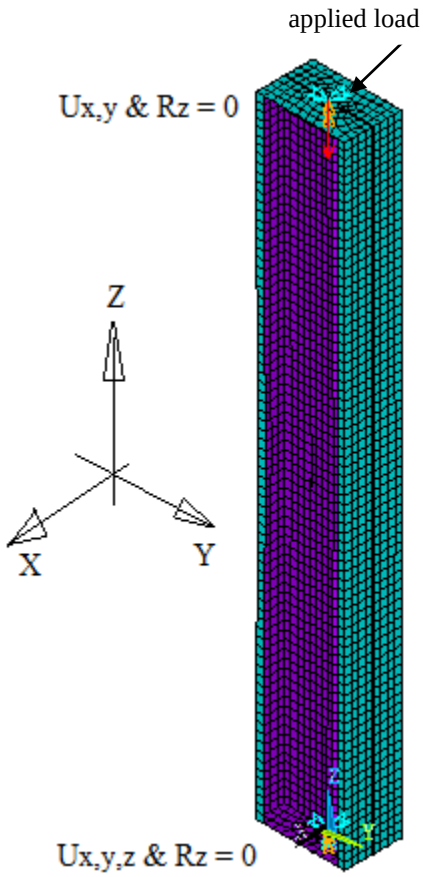

b) Mesh, Boundary Condition, Loading

Figure 7: Finite element model

The end conditions for column elastic line are treated as pinned condition. However, warping of the end column cross sections is restrained due to the provision of thick end plates. The loaded end prevented from both rotations about z-axis and translations in both X and Y directions. On the other hand, the unloaded end was prevented from translation in the three directions X, Y and Z as well as from rotations about the z-axis. The loads are applied on a node at one end with eccentricities about X, Y axis similar to those measured in the tests, and were incrementally increased through successive load steps. Newton-Raphson iterations were used in solving the nonlinear system of equations. It was noted in El Aghouryet.al., (2014) the ultimate loads are sensitive to the overall geometric imperfection modes rather than local imperfection ones, therefore, the column was modeled with a half-sine wave bending about the minor axis "Y". The imperfection value considered is L/1000, where L is the column length. In-addition, the residual stresses pattern was assumed similar to that demonstrated in Fig. 3.

The numerical model results are plotted in Fig. 4 and Fig. 5 along with the test results for specimens S50-25-50 and S50-25-100; res[ectively. Generally, there is good agreement between

the experimental and numerical results. In addition, the finite element ultimate loads of all specimens are listed in table 3. Note that, P_{u2} represents the ultimate loads without eccentricities. Close observation to the results indicate that there is certain increase in the ultimate loads by increasing the ratio a/B. To add on, the effect of spacing between connectors is very important. Therefore, the ultimate loads of specimens S50-25-50 and S50-25-100 are determined for different intervals between connectors. In specimen S50-25-100, P_u = 63.7 KN and 63.8KN when the connectors are placed at intervals of L/4 and L/6; respectively. Similarly, the ultimate loads of specimen S50-25-50 is equal to 112.6 KN when the connectors are placed at intervals of L/4. By comparing these results with those in Table 3, we can conclude that the ultimate loads are not significantly changed by varying the spacing between connectors.

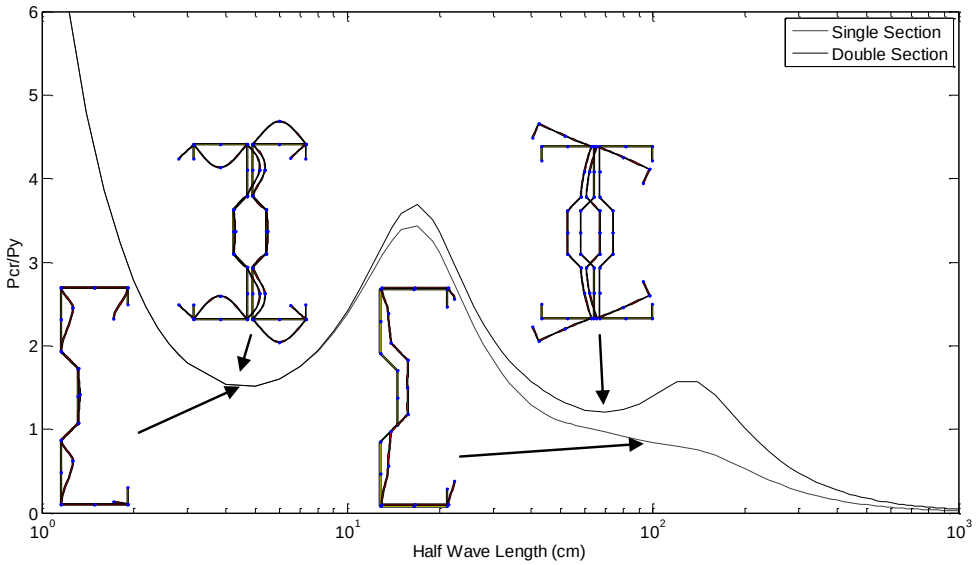

Figure 8: Elastic buckling loads of the S50-25 section

It may be interesting to highlight the elastic buckling behavior of the combined sigma section as basis of assessing the capabilities of DSM Schafer (2002) to predicate the ultimate loads of such sections. The critical buckling loads of the studied sections have been calculated using CUFSM computer program. In the model, the nodal lines that correspond to the bolts location are constrained together. This modeling assumed that the webs of the two sections are connected along the whole length of the columns. Results are depicted in Figs. 7 and 8 for wide flange sections (B = 50) that have ratios of a/B = 0.25 and 0.75; respectively. It is noted that, increasing the ratio a/B pushing both the critical local and distortional buckling loads up, and reducing the critical distortional half wave length. It is worth noting that the critical distortional half wave length is 700 mm for section S50-25, and 440 mm for section S50-75, which is close to that measured in the lab. Moreover, for the sake of comparison, findings of single sections are added to the figure. It is observed that, when the sections are connected through the web the critical distortional buckling loads increases and the corresponding critical distortional half wave length decreases. This is clearly shown in sections with large ratios of the inward recess of the middle part of the web to the flange width (a/B = 0.75). The reason of this response may be illustrated as the rotational stiffens of the flange web juncture enhanced when the webs of the two sections are connected.

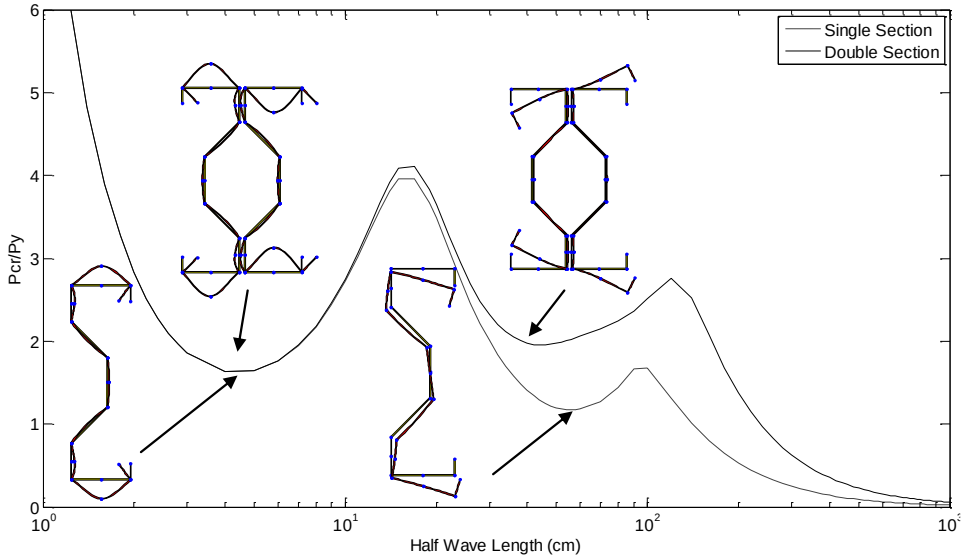

Figure 9: Elastic buckling loads of the S50-75 section

In this section, the experimental ultimate loads, P_u, were compared against predictions from design rules of the Direct Strength Method "*DSM*" by Schafer (2002),as well as the *AISI-2012* equations. The elastic buckling loads determined by CUFSM program are employed in the calculation of the DSM, in which the ultimate loads are defined as the minimum of the local, distortional, and the overall ultimate loads. In *AISI-2012*, the ultimate loads are calculated based on the effective area concept. In-addition, the distortional buckling strength, P_{nd}, according to provision C4.2, AISI-2012 are determined and added to the figure. The partial safety factors, γ_{M1} and ϕ_c, were not included when calculating the design loads.

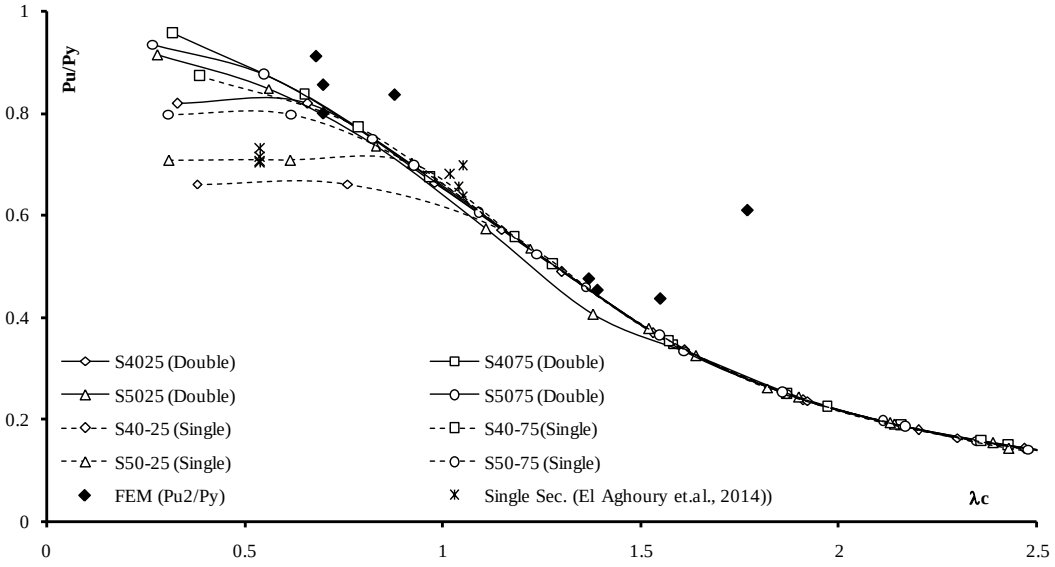

Figure 10 Comparison of the results with the predicted values of DSM

The design loads calculated according to DSM and *AISI-2012* are plotted as function of the normalized slenderness ratio, $\lambda_c = \sqrt{F_y/F_e}$ in Fig.10 and Fig. 11; respectively. It is clear that both

DSM and AISI-2012 are conservatively predicate the ultimate loads of the combined sections. In addition the distortional buckling loads, P_{nd}, determined by AISI-2012 provision C4.2 provides very lower limit. Again, the results are compared with that of single section. It conspicuous that, the DSM is more sensitive than AISI-2012 to the modifications in the distortional loads between single and combined sections.

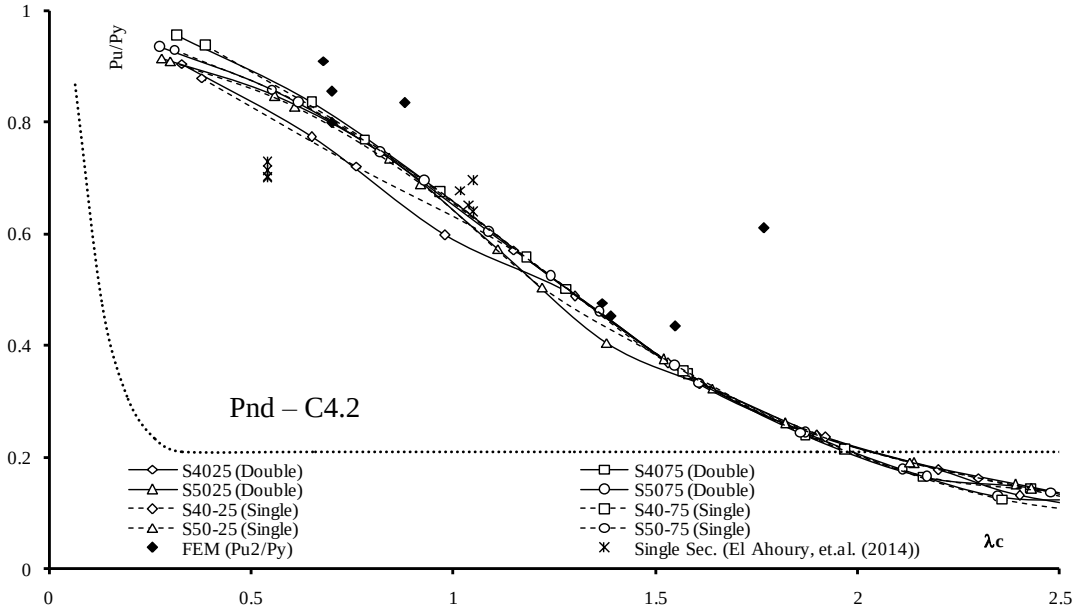

. Figure 11: Comparison of the results with the predicted values of AISI-2012

4. Conclusions

In this paper the axial strength of columns consists of back to back cold formed sigma sections has been investigated experimentally and numerically. In the tests, it is found that the failure modes of short columns were governed by flange distortional buckling. However, in intermediate height columns the failure mode is the interactive overall distortional buckling. In addition, the finite element model failure shapes are comparable with the test results, and the distortional buckling half wave length are very close to that measured in the lab. Further, numerical results revel that the ultimate loads are not significantly changed by varying the spacing between connectors. Moreover, increasing ratios of the inward recess of the middle part of the web to the flange width, a/B, pushing both the local and distortional buckling loads up, and reducing the critical distortional half wave length. Besides, the rotational stiffens of the flange web juncture enhanced when the webs of the two sections are connected together. This leads to increase the critical distortional buckling loads and decreases the corresponding half wave length, compared with that of the single sigma sections. Eventually, results are compared with the predicted strength of *AISI-2012*, and the *DSM*. Comparison showed that the design specifications conservatively predict the ultimate loads. In addition, *DSM* is more sensitive to the variation in the distortional buckling loads between single and combined sections.

References

AISI (2012), Cold-formed steel design manual, American Iron and Steel Institute, AISI

ASTM A370, "Standard Test Methods and definitions for mechanical testing of steel products".

ANSYS, Version 12.0.1, Swanson Analysis Systems, Houston, PA. Desalvo, G.J., and Gorman, R.W.,

Andrzej Garstecki, Witold Kakol, Katarzyna Rzeszut, (2002) "Classifications of local-sectional geometric imperfections of steel thin-walled cold-formed sigma members" *Publishing House of Poznan University of Technology*, Poznań

CUFSM V3.12, "Elastic Buckling Analysis of Thin-Walled Members by Finite Strip Analysis", http://www.ce.jhu.edu/bschafer/cufsm

D.J Klingshirn, E. A. Sumner, and N. A. Rahman, (2010) "Experimental Investigation of Optimized Cold-Formed Steel Compression Member" *Twentieth International conference on cold formed steel structures*, St. Louse, Missouri, U.S.A., November 3&4.

David C. Fratamic, Shahabeddin Torabian, Benjamin W. Schafer, (2015) "Composite Action in Global Buckling of Built-Up Columns Using Semi-Analytical Fastener Elements" *Proceedings of the Annual Stability Conference Structural Stability Research Council* Nashville, Tennessee, March 24-27.

Fadhluhartini Muftah, Mohd Syahrul Hisyam Mohd Sani1, Mohd Fakri Muda, and Shahrin Mohammad, (2014) "Assessment of Connection Arrangement of Built-up Cold-formed Steel Section under Axial Compression" *Advanced Materials Research* ,1043, pp 252-257.

H.H. Lau and T.C.H. Ting, (2009) "An Investigation of The Compressive Strength of Cold-Formed Steel Built-Up I Sections" *Proceedings of Sixth International Conference on Advances in Steel Structures* , Hong Kong, China.

Mohamed El Aghoury, Maged Tawfick Hanna and Essam Amoush, (2014) " Effect of Initial Imperfections on Axial Strength of Cold Formed Steel Single Lipped Sigma Section" *EUROSTEEL 2014*, Naples, Italy, September 10-12.

M..El Aghoury, A.H. Salem, M.T. Hanna and E.A. Amoush, (2010). "Experimental Investigation for the Behaviour of Battened Beam- Columns Composed of Four Equal Slender Angles", *Thin-Walled Structures*, 48 (9), pp. 669-683.

Schafer BW, (2002) "Design Manual for the Direct Strength Method of Cold-formed Steel Design", Final Report to the American Iron and Steel Institute, Washington, DC.

Thomas H. K. Kang, Kenneth A. Biggs, and Chris Ramseyer (2013) "Buckling Modes of Cold-Formed Steel Columns", *IACSIT International Journal of Engineering and Technology*, 5(4).